Behaviour of trace elements in arsenian pyrite in ore deposits

Artur P. Deditius*, Stephen E. Kesler, Rodney C. Ewing,
Department of Geological Sciences, University of Michigan, 2534 C.C. Little Bldg, Ann Arbor, MI 48109-1005, USA
*Present address: CSIRO Exploration and Mining, 26 Dick Perry Ave., Kensington, Perth, WA 6151, Australia

Satoshi Utsunomiya
Department of Chemistry, Kyushu University, Ropponmatsu 4-2-1, Chuo-ku, Fukuoka-Shi, 810-8560, Japan

John Walshe
CSIRO Exploration and Mining, 26 Dick Perry Ave., Kensington, Perth, WA 6151, Australia

Abstract. As-bearing pyrite is one of the main hosts for Au and other trace elements in epithermal, Carlin and mesothermal (orogenic) Au deposits. A review of our own and published SIMS, EMPA, LA-ICP-MS and PIXE analyses of pyrite from these deposits suggests that the solubility of Ag, Te, Hg, Sb and Pb in arsenian pyrite is controlled by As-content in a manner similar to that previously reported for Au by Reich et al., (2005). The trace elements can be divided into two groups that exhibit different solubility limits: i) Au, Ag, Te, Hg and Bi ii) Sb and Pb. HRTEM and HAADF-STEM observations reveal nanoparticles with compositions of Sb-As-Fe-Ni, Sb-Pb-Te, Pb-Bi, PbS and Ag in arsenian pyrite above the solubility limit. Most nanoparticles are between 5 and 200 nm, with some containing Pb reaching 500 nm. Pyrite from Carlin-type and epithermal deposits contains larger amounts of Sb and/or As than pyrite from higher-temperature orogenic gold/mesothermal deposits. This suggests that the solubility of trace elements in pyrite appears to decrease with increasing temperature.

Keywords: Arsenian pyrite, trace elements, solubility, geochemistry, ore deposits

1 Introduction

Pyrite is the main, and sometimes the only, common sulphide mineral in many low and moderate-temperature ore deposits. Trace element contents and zoning in pyrite, whether of the growth or sectoral type, provide useful information about the compositional evolution of the mineralizing fluids that formed the deposits. Information on the trace element content of pyrite helps to i) recognize the sequence of pulses and the chemistry of the hydrothermal fluids (e.g., Large et al., 2007; Deditius et al., 2009b; accepted); ii) identify the nature of the Au+Ag complexing agents, (i.e., Te-complexes may enhance the incorporation of Au and Ag into pyrite; e.g., Pals et al., 2003; Kesler et al. 2007).

Arsenic is the most abundant and thus most important minor element that is incorporated into pyrite in most hydrothermal ore deposits, and it has an important control on incorporation of Au. Reich et al. (2005) have shown that the concentration of Au in pyrite is related to the arsenic content. Additional elements that are found in pyrite include Ag, Sb, Te, Se, Pb, Bi, Hg, Cu, Zn, Ni and Co, and their compositional ranges and relation to As remain poorly understood.

There is also very little information on the form of the trace elements in the pyrite structure. Are they present in solid solution or as nanoparticles that are "invisible" to analyses by secondary ion-mass spectrometry (SIMS), laser-ablation inductively coupled mass spectrometry (LA-ICP-MS), and electron microprobe analysis (EMPA)? Another important aspect is the oxidation state of the trace elements. This is important in distinguishing between possibilities for monovalent and coupled substitutions in pyrite. The most investigated element, gold, has been found to occur as Au^0 and Au^{1+}, although Au^{3+} has also been suggested (Chouinard et al., 2005). The oxidation state of As was determined to be As^{1-} and As^{3+}, utilizing X-ray absorption near-edge structure (XANES) and X-ray photoelectron spectroscopy (XPS), respectively (Simon et al. 1999, Deditius et al. 2008). The most recent studies also revealed amorphous As-Fe-S nano-inclusions in arsenian pyrite, which suggest that As may occur as the native element in pyrite (Deditius et al., 2009a).

This report examines the solubility limits of trace elements including Ag, Te, Sb, Pb, Bi, Hg, Cu, Zn, Co, Ni and Se in pyrite, with particular attention to their concentration as a function of increasing As-content. The compilation of published and new SIMS, LA-ICP-MS, EMPA analyses is supplemented by nano-scale observations using high-angle annular dark-field scanning transmission electron (HAADF-STEM) and high-resolution (HRTEM) microscopy. We also evaluate the relation of these trace elements to the Au-content of pyrite. Pyrites included in this study are from orogenic gold and other mesothermal deposits, as well as low- and high-sulfidation epithermal deposits and Carlin deposits (Table 1). The behaviour of these trace elements as a function of temperature is also investigated.

Name of the deposit	Type	References
Yanacocha	E	Deditius et al. (2008)
Pueblo Viejo	E	Deditius et al. (accepted)
Carlin-type	E	Emsbo et al. (2003); Reich et al. (2005); new analyses;
Emperor	E	Pals et al. (2003)
North Arm	E	Griffin et al. (1991)
Sukhoi Log	OG	Large et al. (2007)
Bendigo-Stawell zone	OG	Wood and Large (2007)
Roudný	M	Zachariáš et al. (2004)

2 Relations and geologic setting of trace elements in arsenian pyrite

When considered as a single data set, analyses from all of the deposits in Table 1 show a generally positive correlation of Sb with Au, Ag, Hg and Cu, and of Te with Au and Ag. Lead correlates positively with Sb in orogenic gold deposits. Only Carlin-type deposits show a positive correlation between Au and Se. Bismuth correlates positively with Pb, and Co correlates with Ni in all analysed samples. These general trends agree with previous observations indicating that As has a positive correlation with Se and Cu (Griffin et al. 1991); Pb with Bi and Au with Sb (Wood and Large 2007); Sb with Pb (Morey et al. 2008); Au with Ag, Au with Cu, Pb and Te (Pals et al. 2003; Large et al. 2007).

The chemical state and form of gold in the matrix of arsenian pyrite at nanoscale levels have been discussed by Palenik et al. (2004) and Reich et al. (2005). New HAADF-STEM and HRTEM observations reveal that some of the trace elements in arsenian pyrite form nanoparticles which differ in their chemical composition and size. Pyrite from Pueblo Viejo has nanoinclusions of Sb-Pb-Te (~100nm in size), and Pb-Bi (20x100nm elongated inclusions) that are surrounded by polycrystalline pyrite. Carlin-type deposits contain nanoinclusions of Fe-Sb-As-Ni, PbS and Ag (Fig. 1a) that measure 50-200nm, 200-500nm and 5-50nm, respectively, were found in pyrite. Silver forms the smallest nanoparticles in arsenian pyrite, 5-50 nm, the same size as reported for native Au 5-50 (Reich et al. 2006). These observations suggest that native metals form the smallest particles, followed by larger sulfosalts/amalgams, and sufides form the largest crystals in the matrix of As-pyrite. The combination of TEM analyses with SIMS and EMPA data are the basis for our proposal of several different solubility limits for the trace elements in arsenian pyrite, for example Sb (Fig. 1b).
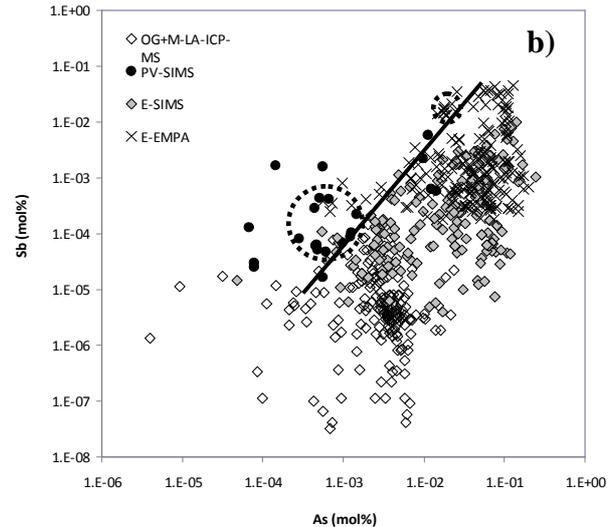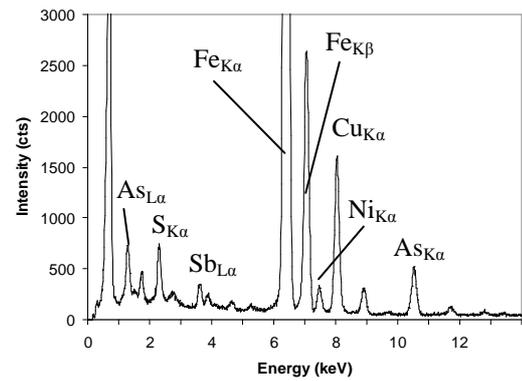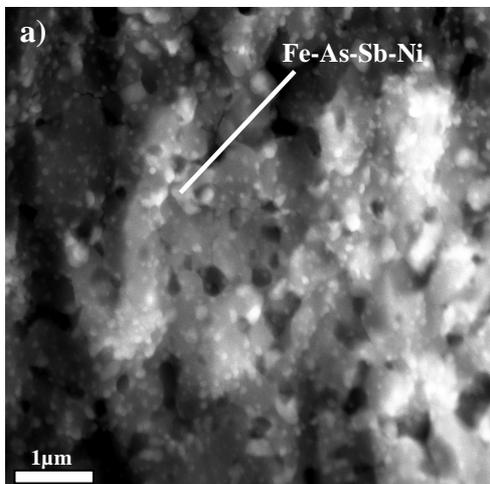

Figure 1. a) HAADF-STEM image of Fe-Sb-As-Ni nanoparticles in arsenian pyrite from Carlin-type (Lone Tree) deposit associated with TEM-EDX spectrum; Note the low contents of S in nanoparticles; b) suggested solubility limit for Sb in arsenian pyrite as a function of As-content. Analytical points in doted circles represent: i) small circle – EMPA and ii) larger SIMS. Abbreviations as in Table 1.

3 Solubility of trace elements in arsenian pyrite

We interpret these relations to indicate that arsenic facilitates the incorporation of trace elements, (in addition to Au) into the pyrite structure. This is due to the structural distortion and/or charge imbalance that is created when As substitutes for sulphur or iron or even when it is present in a zero-valent state (e.g., Fleet and Mumin 1997; Reich et al. 2005; Deditius et al. 2008, 2009). The divalent Co and Ni and to a lesser extent Zn and mono/divalent Cu have limited solid solution in pyrite, substituting for Fe (Makovicky 2006; and references therein).

Concentration limits for Ag, Te, Hg, Pb, Bi and Sb in arsenian pyrite appear to be similar to those for Au, with respect to the slope of the line illustrated on Fig. 1b. However, concentration limits for Pb and Sb are one order of magnitude higher than the limit for Au, Ag, Te and Hg. The lack of adequate EMPA analyses of Bi and the presence of Pb-Bi nanoparticles in arsenian pyrite prevent efforts to identify an upper limit for Bi.

The temperature of precipitation controls the

amounts of trace elements that are soluble in arsenian pyrite and thus the occurrence and the size of nanoparticles. In heating experiments of natural arsenian pyrite from low-temperature Carlin-type deposit, Au nanoparticles <2nm in size dissolve at temperatures ~370°C, and the Au migrates to accumulate as larger particles, ~8nm in size (Reich et al. 2006). How this process operates under natural conditions is not known, in part because there are no TEM data for nanoparticles in pyrite from higher temperature systems such as orogenic gold deposits. The reported coarsening of the larger nanoparticles with increasing temperature (Reich et al. 2006) may be responsible for the observed decrease in the concentration of Au, Ag, Sb, Pb and Te in the arsenian pyrite under mesothermal conditions. This would be due to exsolution and precipitation of their own mineral phases as suggested by Mumin et al. (1994) and Large et al. (2007).

3 Conclusions

The concentration of Au, Ag, Te, Sb, Pb, Bi and Hg increases in arsenian pyrite as a function of increasing As-content. Concentrations of these elements also appear to decrease with increasing temperature of deposition for pyrite. Copper, Co, Ni and Zn do not show concentration limits in pyrite with respect to As-content. HAADF-STEM and TEM-EDX analyses of various types of nanoparticles reveal that they differ in size and chemical composition. The size of most nanoparticles of metals and amalgams vary from ~5-200nm, and PbS forms crystals larger than 200 nm. We proposed that the measured concentration limits represent solubility limits that can be used to distinguish between analyses of the trace elements in arsenian pyrite, that reflect the solid-solution, *versus* those that contain nanoparticles.

Acknowledgements

References

Chouinard A, Paquette J, Williams-Jones AE (2005) Crystallographic controls on trace-element incorporation in auriferous pyrite from Pascua epithermal high-sulfidation deposit, Chile-Argentina: Canadian Mineralogist 43: 951-963.

Cline JS, Hofstra AH, Muntean JL, Tosdal JM, Hickey KA (2005) Carlin-type gold deposits in Nevada: Critical geologic characteristics and viable models: Economic Geology 100th Anniversary Volume: 451-484.

Deditius AP, Utsunomiya S, Renock D, Ewing RC, Ramana CV,

Becker U, Kesler SE (2008) A proposed new type of arsenian pyrite: Composition, nanostructure and geological significance: Geochimica et Cosmochimica Acta 72: 2919-2933.

Deditius AP, Utsunomiya S, Ewing RC, Kesler SE (2009a) Nanoscale "liquid" inclusions of As-Fe-S in arsenian pyrite: American Mineralogist 94: 391-394.

Deditius AP, Utsunomiya S, Ewing RC, Chryssoulis SL, Venter D, Kesler SE (2009b) Decoupled geochemical behavior of As and Cu in hydrothermal systems: Geology (accepted).

Fleet ME, Mumin AH (1997) Gold-bearing arsenian pyrite and marcasite and arsenopyrite from Carlin Trend gold deposits and laboratory synthesis: American Mineralogist 82: 182-193.

Goldfarb RJ, Baker T, Dubé B, Groves DI, Hart CJR, Gosselin P (2005) Distribution, character and genesis of gold deposits in metamorphic terranes: Economic Geology 100th Anniversary Volume: 407-450.

Griffin WL, Ashley PM, Ryan CG, Sie SH, Suter GF (1991) Pyrite geochemistry in the North Arm epithermal Ag-Au deposit, Queensland, Australia: A proton-microprobe study: Canadian Mineralogist 29: 185-198.

Kesler SE, Deditius AP, Chryssoulis SL (2007) Geochemistry of Se and Te in arsenian pyrite: New evidence for the role of Se and Te hydrothermal complexes in Carlin and epithermal-type deposits: Geological Survey of Finland Guide 53: 57-60.

Large RR, Maslennikov VV, Robert F (2008) Multistage sedimentary and metamorphic origin of pyrite and gold in the giant Sukoi Log deposit, Lena Gold Province, Russia: Economic Geology 102: 1223-1267.

Makovicky E (2006) Crystal structures of sulfides and other chalcogenides: Review in Mineralogy and Geochemistry 61: 7-125.

Mumin AH, Fleet ME, Chryssoulis SL (1994) Gold mineralization in As-rich mesothermal gold ores of the Bogosu-Prestea mining district of the Ashanti Gold Belt, Ghana: Remobilization of the "invisible" gold: Mineralium Deposita 29: 445-460.

Palenik CS, Utsunomiya S, Reich M, Kesler SE, Ewing RC (2004) "Invisible" gold revealed: direct imagining of gold nanoparticles in a Carlin-type deposit: American Mineralogist 89: 1359-1366.

Pals DW, Spry PG, Chryssoulis SL (2003) Invisible gold and tellurium in arsenic-rich pyrite from the Emperor gold deposit, Fiji: Implications for gold distribution and deposition: Economic Geology 98: 479-493.

Reich M, Kesler SE, Utsunomiya S, Palenik CS, Chryssoulis SL, Ewing RC (2005) Solubility of gold in arsenian pyrite: Geochimica et Cosmochimica Acta 69: 2781-2796.

Reich M, Utsunomiya S, Kesler SE, Wang LM, Ewing RC, Becker U (2006) Thermal behaviour of metal nanoparticles in geologic materials: Geology 34: 1033-1036.

Simon G, Huang H, Penner-Hahn JE, Kesler SE, Kao LS (1999) Oxidation state of gold and arsenic in gold-bearing arsenian pyrite: American Mineralogist 84: 1071-1079.

Wood BL, Large RR (2007) Syngenetic gold in western Victoria: occurrence, age and dimensions: Australian Journal of Earth Sciences 54: 711-732.

Zachariáš L, Frŷda J, Paterova B, Mihaljevič B (2004) Arsenopyrite and As-bearing pyrite from the Roudný deposit, Bohemian Massif: Mineralogical Magazine 68: 31-46.